Biochemical Pharmacology, Vol. 58, pp. 503–515, 1999.

ELSEVIER

ISSN 0006-2952/99/$–see front matter
PII S0006-2952(99)00117-3

Characterization of O,O-Diethylphosphoryl Oximes as Inhibitors of Cholinesterases and Substrates of Phosphotriesterases

Haim Leader, Adam Vincze,* Bracha Manisterski,* Nathan Rothschild,† Carlos Dosoretz† and Yacov Ashani*‡*

*Israel Institute for Biological Research, Ness-Ziona, Israel; and †MIGAL-Galilee Technological Center, Kiryat Shmona, Israel

ABSTRACT. Reactivators of organophosphate (OP)-inhibited cholinesterases (ChEs) are believed to give rise to phosphorylated oximes (POX) that reinhibit the enzyme. Diethylphosphoryl oximes (DEP-OX) that were generated *in situ* were demonstrated in the past to be unstable, yet were more potent inhibitors of acetylcholinesterase (AChE) than the parent OPs. In view of the inconsistencies among reported results, and the potential toxicity of POXs, it seemed important to characterize authentic DEP-OXs, and to evaluate their interference with reactivation of diethylphosphoryl-ChE (DEP-ChE) conjugates. To this end, the diethylphosphoric acid esters of 1-methyl-2-pyridinium carboxaldehyde oxime (DEP-2PAM) and 1-methyl-4 pyridinium carboxaldehyde oxime (DEP-4PAM) were synthesized and chemically defined. The half-lives of DEP-2PAM and DEP-4PAM in 10 mM Tris buffer, pH 7.8, at 29° were found to be 10 and 980 sec, respectively. The two DEP-OXs inhibited ChEs with the following ranking order: for DEP-2PAM, human butyrylcholinesterase (HuBChE, $k_i = 2.03 \times 10^9\ M^{-1}\ min^{-1}$) > mouse AChE (MoAChE) ≅ fetal bovine serum AChE (FBS-AChE) ≅ equine BChE (EqBChE); for DEP-4PAM, HuBChE ($k_i = 0.71 \times 10^9\ M^{-1}\ min^{-1}$) > EqBChE > MoAChE > FBS-AChE. A dialkylarylphosphate hydrolase (phosphotriesterase; PTE) from *Pseudomonas* sp. catalyzed the hydrolysis of DEP-4PAM with $k_{cat}/K_m = 3.56 \times 10^7\ M^{-1}\ min^{-1}$ and $K_m = 0.78$ mM. Reactivation of DEP-ChEs was enhanced by PTE when 4-PAM-based oximes were used as reactivators, whereas reactivation with 2-PAM-based oximes was not affected by PTE. This observation is attributed primarily to the short half-life of DEP-OXs derived from the latter oximes. Relatively low doses of PTE can detoxify large quantities of DEP-OXs rapidly, and thereby augment the efficacy of antidotes that contain the oxime function in position 4 of the pyridine ring. BIOCHEM PHARMACOL **58**;3:503–515, 1999. © 1999 Elsevier Science Inc.

KEY WORDS. organophosphate; oximes; inhibition; reactivation; acetylcholinesterase; butyrylcholinesterase; phosphotriesterase; detoxification

Reactivation of OP§-inhibited ChE by quaternary oximes is believed to proceed via a substitution reaction that causes a transient accumulation of phosphonylated or POX intermediates (Fig. 1a). The possibility of reinhibition of AChE (EC 3.1.1.7) by POXs was proposed by Wilson and Ginsburg [1], who suggested the formation of a potent anti-ChE compound that caused an approach to equilibrium rather than complete reactivation during reaction of a diethylphosphoryl-AChE conjugate with 2-PAM. POXs can also be generated by a direct reaction between the oximes and the OPs themselves (Fig. 1b). For example, methylphosphonylated oximes obtained *in situ* by reacting isopropyl methylphosphonofluoridate (sarin) [2–5] or pinacolyl methylphosphonofluoridate (soman) [5, 6] with a variety of quaternary oximes were estimated to be 10- to 100-fold more potent inhibitors of AChE than sarin or soman. These observations point to the dependence of both the stability and anti-ChE activity of methylphosphonylated oximes on the type of reactivator used (mono- or bis-quaternary oxime), and on the position of the oxime function in the pyridinium ring. A recent investigation on the acceleration of reactivation by quaternary ligands that are devoid of

‡ Corresponding author: Dr. Y. Ashani, Israel Institute for Biological Research, P.O. Box 19, Ness-Ziona, Israel. Tel. 972-8-9381455; FAX 972-8-9381548; E-mail: yacov@iibr.gov.il

§ *Abbreviations*: OP, organophosphate; POX, phosphoryl oxime; DEP-OX, diethylphosphoryl oxime; DEP-2PAM, *O*-(*O*,*O*-diethylphosphoryl)-1-methyl-2-pyridinium carboxaldehyde oxime methyl sulfate; DEP-4PAM, *O*-(*O*,*O*-diethylphosphoryl)-1-methyl-4-pyridinium carboxaldehyde oxime methyl sulfate; ChE, cholinesterase; AChE, acetylcholinesterase; BChE, butyrylcholinesterase; HuBChE, human butyrylcholinesterase; MoAChE, mouse acetylcholinesterase; FBS-AChE, fetal bovine serum acetylcholinesterase; EqBChE, equine butyrylcholinesterase; PTE, phosphotriesterase; 2-PAM, 1-methyl-2-pyridinium carboxaldehyde oxime iodide; P2S, methyl sulfonate salt of 2-PAM; 4-PAM, 1-methyl-4-pyridinium carboxaldehyde oxime iodide; HI-6, [1-(2′-carboxaldehyde oxime-1′-pyridinium)-3-(4′′-carbamoyl-1′′-pyridinium)-2-oxybis-methylene dichloride]; HLö7, 1-(2′,4′-bis-carboxaldehyde oxime-1′-pyridinium)-3-(4′′-carbamoyl-1′′- pyridinium)-2-oxybis-methylene diiodide; DEPQ, 7-(*O*,*O*-diethylphosphinyloxy)-1-methylquinolinium methyl sulfate; DEPC, *O*,*O*-diethyl phosphorochloridate; DMSU, dimethyl sulfate; AT, ambient temperature; 2-CNPY, 2-cyano-1-methylpyridinium methyl sulfate; and 4-CNPY, 4-cyano-1-methylpyridinium methyl sulfate.

Received 24 August 1998; accepted 2 December 1998.

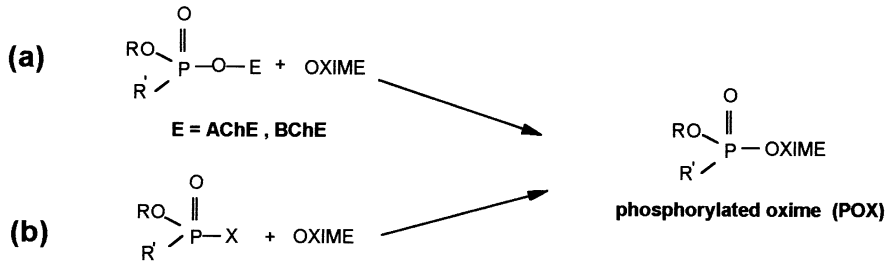

R=C_2H_5 , iC_3H_7 , pinacolyl ; R' =CH_3 , OC_2H_5 ; X=F, *p*-nitrophenyl, $SCH_2CH_2NR_2$

OXIME

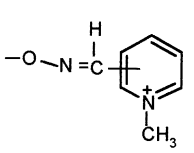

	Oxime position
2-PAM	2
4-PAM	4

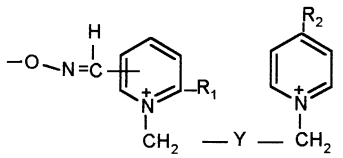

	Oxime position	R_1	Y	R_2
TMB-4	4	H	CH_2	CH=NOH
toxogonin	4	H	O	CH=NOH
HI-6	2	H	O	$CONH_2$
HLo7	4	CH=NOH	O	$CONH_2$

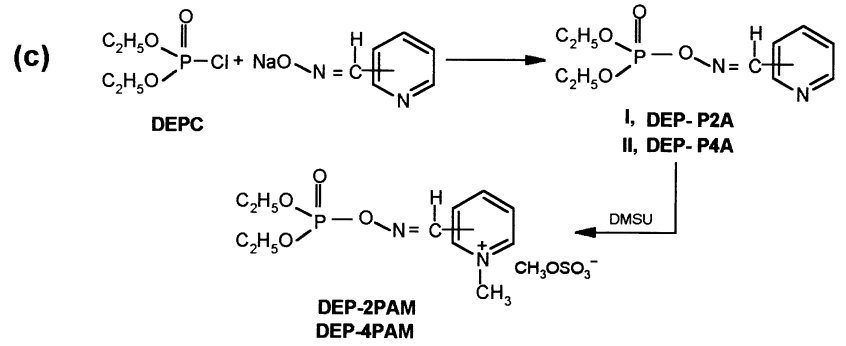

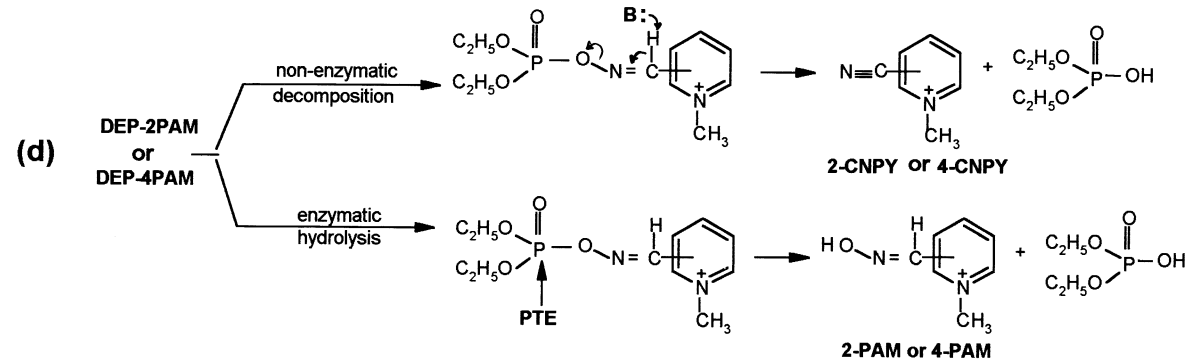

FIG. 1. Reaction pathways and structures of compounds that are involved in the formation and decomposition of phosphorylated oximes. (a) Formation of POXs during reactivation. (b) Generation of POXs from OPs and oximes. (c) Synthesis of DEP-2PAM and DEP-4PAM. (d) Mechanism of decomposition and hydrolysis of DEP-POXs. Upper pathway, Beckman elimination. Lower pathway, substitution reaction at the phosphorus atom.

nucleophilic activity provided indirect evidence in support of such a relationship [7].

In situ formation of toxic POXs was also implied from experiments with various *O,O*-diethylphosphates that were reacted with oxime reactivators [4, 5].

The conceivable generation of POXs during oxime treatment of OP intoxication is of considerable importance for the therapeutic management of pesticide poisoning. A large number of widely used phosphorothioates (e.g. parathion, chlorpyriphos, diazinon) are oxidized *in vivo* to potent DEP-based inhibitors of AChE and BChE (EC 3.1.1.8). Inhibition of either enzyme can be reversed by quaternary oximes, provided that the circulating OP metabolite(s) does not exceed a level that causes significant reinhibition of the reactivated enzyme. Hence, oxime therapy with antidotes such as P2S strongly depends on the persistence of the anti-ChE activity in blood [8]. Accumulation of POXs might interfere with oxime reactivation in a manner analogous to the anti-ChE OP metabolites. POXs are toxic compounds, and in one case it was noted that the median lethal dose (LD_{50}) of a POX obtained from sarin and 4-PAM was 0.2 mg/kg (mice, i.v.) [9]. A recent study suggested that combined therapy with P2S and PTE (organophosphate hydrolase, EC 3.1.8.1) can significantly improve clinical recovery after intoxication with *O,O*-diethylphosphate-based pesticides [10]. It was rationalized, on the basis of structural similarities among certain OP substrates, that in addition to detoxification of OPs, therapy with PTE may also benefit from enhanced detoxification of POXs [10]. However, no direct evidence was available to support the hypothesis that POXs are substrates of PTE.

Essentially, two approaches were applied in the past for the *in situ* evaluation of *O,O*-diethylphosphoryl oximes: (a) by monitoring the time course of the anti-ChE activity of aqueous solutions of OPs and oximes [4, 5], and (b) from measurements of the rate of reactivation of diethylphosphoryl-AChE conjugates (DEP-AChE) [11]. However, the two procedures provided different second-order rate constants of AChE inhibition. Furthermore, conclusions with respect to the stability of POXs were in marked disagreement. To obtain direct data on the biochemical properties of DEP-OXs, the diethylphosphoric acid esters of 2-PAM (DEP-2PAM) and 4-PAM (DEP-4PAM) (Fig. 1) were synthesized and characterized as inhibitors of AChEs and BChEs, and as substrates of a PTE purified from *Pseudomonas* sp. Results provided an explanation for the differences in the potency of certain oxime reactivators and facilitated the examination of the potentiality of PTEs as a catalytic scavenger of phosphorylated oximes.

MATERIALS AND METHODS

2- and 4-pyridine carboxaldehyde oximes (P2A and P4A, respectively), 2- and 4-cyanopyridines, 4-PAM, 1,1′-trimethylene bis-(4-carboxaldehyde oxime)-pyridinium dibromide (TMB-4), DMSU, and DEPC were obtained from the Aldrich Chemical Co. DEPC was distilled before use. *O,O*-Diethyl *p*-nitrophenylphosphate (paraoxon), 2-PAM and its methyl sulfonate salt P2S, and *N*-(2-acetamido)iminodiacetic acid (ADA buffer) were purchased from the Sigma Chemical Co. Toxogonin [1,1′-oxybis-methylene bis-(4-carboxaldehyde oxime)-pyridinium dichloride] was obtained from the Merck Co. HI-6 and HLö7 were obtained from Dr. G. Amitai. The inhibitor DEPQ was prepared as described elsewhere [12].

^{1}H, ^{31}P, and ^{13}C NMR spectra were recorded with a GN 300WB NMR instrument (General Electric) at AT. For specific details see below and Table 1.

Mass spectra were recorded with a VG-Micromass model VSEQ sector instrument interfaced to an HP5890 gas chromatograph and operated by a Vax Station 3000 computer, using VG's OPUS version 3.2 software. Spectra of quaternary compounds were determined by using liquid single ion mass spectroscopy (SIMS) with appropriate ion source and a Cs ion gun.

DEP-2PAM and DEP-4PAM were synthesized as outlined in Fig. 1c, as described below.

DEP-2PAM

The tertiary phosphorylated oxime precursor (Fig. 1c, I) was obtained by a modified procedure of van Hooidonk *et al.* [13]. P2A (6.1 g, 0.05 mol) was dissolved in freshly prepared 1.0 M sodium methoxide solution in methanol (50 mL, containing 2.7 g of $NaOCH_3$), and the pale yellow methanolic solution was evaporated under vacuum to dryness. The remaining sodium salt of P2A was stirred in 200 mL of dry ether for 40 min at AT. The mixture was cooled to 4°, and freshly distilled DEPC (8.6 g, 0.05 mol) in 50 mL of dry ether was added dropwise while maintaining the temperature below 5°. Stirring was continued for 2 hr at AT, and the precipitated NaCl was removed by filtration. The remaining solution was washed with cold water (4°, 2×50 mL), dried over anhydrous $MgSO_4$, and the ether evaporated. ^{31}P and ^{1}H NMR spectra revealed that the residual yellow oil (12.3 g), *O*-(*O,O*-diethylphosphoryl-2-pyridinium carboxaldehyde oxime (I; Fig. 1c), contained *O,O,O′,O′*-tetraethylpyrophosphate (TEPP) and 2-cyanopyridine (~15%, each). The tertiary ester was purified by column chromatography (silica, $CHCl_3$, and 5% MeOH/$CHCl_3$), and the final product (30% yield) was found to contain approximately 4% TEPP. The structure of I was confirmed by ^{1}H, ^{31}P, and ^{13}C NMR spectroscopy (Table 1). By electron impact (EI) mass spectrometry the molecular ion was observed at m/z 258.

The foregoing tertiary POX (I, 0.26 g, ~0.001 mol) was dissolved in 5 mL of CH_3CN (HPLC grade) and mixed with a solution of DMSU (0.75 g, 0.006 mol) in 5 mL of CH_3CN. The completion of the quaternization was monitored by use of ^{31}P NMR. After 7 days at AT, the clear solution was diluted with 100 mL of dry ether and the separated viscous oil was triturated with successive amounts of dry ether until the complete removal of TEPP and excess

TABLE 1. ^{1}H, ^{13}C, and ^{31}P NMR spectroscopy data of tertiary and quaternary POXs

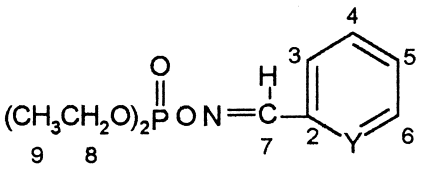

I and DEP-2PAM

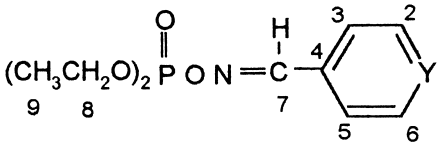

II and DEP-4PAM

Position	I, Y = N			DEP-2PAM, Y = N-CH_3			II, Y = N			DEP-4PAM, Y = N-CH_3		
	^{1}H*	^{13}C†	^{31}P‡	^{1}H*	^{13}C†	^{31}P‡	^{1}H*	^{13}C†	^{31}P‡	^{1}H*	^{13}C†	^{31}P‡
			−3.8 (5 lines)			−4.8 (5 lines)			−3.9 (5 lines)			−4.6 (5 lines)
2		152.4 (s)§			147.5 (s)		8.61 (d)	153.7 (d)		9.04 (d)	149.7 (d)	
3	7.96 (d)	124.5 (d)		8.27 (d)	130.4 (d)		7.47 (d)	124.8 (d)		8.26 (d)	129.0 (d)	
4	7.74 (dd)	139.4 (d)		8.50 (bt)	148.9 (d)			140.5 (s)			148.5 (s)	
5	7.35 (dd)	128.2 (d)		8.08 (bt)	132.9 (d)		7.47 (d)	124.8 (d)		8.26 (d)	129.0 (d)	
6	8.60 (D)	152.6 (D)		9.02 (D)	151.7 (d)		8.61 (d)	153.7 (d)		9.04 (d)	149.7 (d)	
7	8.40 (s)	161.0 (dd)‖		8.97 (s)	154.2 (dd)‖		8.24 (s)	158.7 (dd)‖		8.70 (s)	157.1 (dd)	
8	4.22 (m)	67.6 (t)		4.25 (m)	68.9 (t)		4.19 (m)	68.1 (t)		4.19 (m)	68.6 (t)	
9	1.31 (t)	18.5 (q)		1.35 (t)	19.1 (q)		1.29 (t)	19.2 (q)		1.30 (t)	19.2 (q)	
N—CH_3				4.45 (s)	57.5 (q)					4.47 (s)	57.4 (q)	

*$CDCl_3$, δ (ppm) relative to TMS = 0.0 ppm.
†$CDCl_3$ δ (ppm) relative to $CDCl_3$ = 80.2 ppm.
‡$CDCl_3$ (ppm), negative values indicate up-field shift relative to external 1% trimethyl phosphate in C_6D_6 = 0.0 ppm.
§Letters in parentheses are: (s) singlet; (d) doublet; (t) triplet; (q) quartet; (m) multiplet; (dd) double doublet; and (bt) broad triplet.
‖ Jpc = 16–18 Hz.

DMSU (determined by ^{1}H and ^{31}P NMR spectroscopy). Finally, volatile residues were removed by applying high vacuum. The colorless viscous liquid (DEP-2PAM, 0.22 g, 57% yield) contained ~ 3% diethylphosphoric acid (based on ^{1}H and ^{31}P NMR). ^{1}H, ^{31}P, and ^{13}C NMR spectroscopy confirmed the structure of DEP-2PAM (Table 1). Intact cation at *m/z* 273 was observed in the liquid SIMS. The purity of DEP-2PAM was further confirmed by titration of HuBChE at known concentration, as determined before by use of DEPQ [10, 12], and by the quantitative decomposition of DEP-2PAM to 2-CNPY, as determined by ultraviolet spectroscopy and comparing with authentic 2-CNPY (see below).

DEP-4PAM

The tertiary ester *O*-(*O*,*O*-diethylphosphoryl)-4-pyridinium carboxaldehyde oxime (II; Fig. 1c) was prepared as described above for its 2-substituted isomer, and the crude product (12.3 g yellow oil) was found to be contaminated with TEPP, unreacted P4A, 4-cyanopyridine, and *O*,*O*-diethyl-*O*-methylphosphate. Purification by column chromatography (silica, $CHCl_3$) gave an overall yield of 50% of colorless homogenous oil (^{1}H, ^{31}P, and ^{13}C NMR spectroscopy; Table 1). By EI mass spectrometry the molecular ion was observed at *m/z* 258.

A solution of DMSU (0.63 g, 0.005 mol) in 50 mL of dry ether was added to a solution of the foregoing tertiary ester (II, 1.29 g, 0.005 mol) in 200 mL of dry ether. After several hours at room temperature, the clear solution turned turbid and an oil layer was separated at the bottom of the flask. After 48 hr at AT, the ether was decanted and the remaining viscous oil was stirred and triturated with dry ether (4 × 50 mL). Excess ether was evaporated under vacuum. The structure of the remaining homogenous colorless viscous oil (1.1 g, 57% yield) was shown to be consistent with DEP-4PAM by use of ^{1}H, ^{31}P, and ^{13}C NMR spectroscopy (Table 1). Intact cation at *m/z* 273 was observed in the liquid SIMS. The quantitative release of 4-CNPY in aqueous solutions, and titration of HuBChE at known concentration (for details see Fig. 3C) confirmed the purity of DEP-4PAM.

2-CNPY

DMSU (0.8 g) was added to a solution of 0.25 g of 2-cyanopyridine in 50 mL of dry acetone. The solution was refluxed for 5 hr, cooled to AT, and the crystals that were collected after 24 hr were dried in vacuum over P_2O_5 (0.1 g, 18% yield; m.p. 222–225°, dec.). The structure and purity were verified by UV absorption and NMR spectroscopy: ^{1}H NMR (1% CD_3OD-$CDCl_3$): δ 8.92 (d, J = 6.1 Hz, 1H); 8.40 (t, J = 7.9 Hz, 1H); 8.23 (d, J = 7.9 Hz, 1H); 8.00 (bt, 1H); 4.35 [s, 3H (NCH_3)]; 3.25 [s, 3H (OCH_3)].

4-CNPY

This compound was prepared as described above for the 2-CNPY homologue (0.35 g, 63% yield; m.p. 130–132°).

Its structure and purity were confirmed by UV absorption and NMR spectroscopy: ^{1}H NMR (1% CD_3OD-$CDCl_3$): δ 9.07 (d, J = 6.3 Hz, 2H); 8.24 (bd, J = 6.3 Hz, 2H); 4.4 [s, 3H (NCH_3)]; 3.56 [s, 3H (OCH_3)].

PTE from *Pseudomonas* sp. was purified as previously described [10]. Purified recombinant wild-type MoAChE, and purified FBS-AChE were donated by Professor P. Taylor and Dr. Z. Radic (University of California), and by Dr. B. P. Doctor (Walter Reed Army Institute of Research). HuBChE was purified by procainamide-Sepharose 4B gel affinity chromatography [14], and partially purified EqBChE was purchased from Biozyme Laboratories International Ltd. Active-site concentrations of AChEs and BChEs were determined by titration with DEPQ [12]. Unless otherwise indicated, all enzyme stock solutions were made in 10 mM Tris buffer, pH 7.8, containing 0.1% BSA.

Enzyme Assays

The release of *p*-nitrophenol (at 400 nm) from 1 mM paraoxon in 50 mM phosphate buffer, pH 8.0, at 25°, was used to standardize PTE stock solutions (1060 U/mg). PTE-catalyzed hydrolysis of DEP-2PAM and DEP-4PAM was determined in 10 mM Tris, pH 7.8, at 29°, by monitoring the release of 2-PAM and 4-PAM at 336 nm. The amount of oxime released was calculated from the molar absorbance coefficient of the two oximes in the same buffer. The activities of AChE and BChE were determined by the method of Ellman *et al.* [15], using 0.5 mM acetylthiocholine iodide and butyrylthiocholine iodide, respectively. Assays were carried out in 50 mM phosphate buffer, pH 8.0, at 25°.

Determination of the Inhibition Rate Constants of AChE and BChE

Standard stock solutions of POX (0.1 to 10 μM) were freshly prepared in deionized water adjusted to pH 4.5 by a few drops of 0.1 M acetate buffer, and kept in an ice-water bath. At time zero, POX was diluted into a ChE solution (0.2 to 2 nM) in 10 mM Tris buffer, pH 7.8, containing 0.1% BSA, and incubated at 29°. The final concentrations of the inhibitors were sufficiently high to establish a pseudo-first-order reaction condition. At selected time intervals, aliquots were diluted into Ellman's assay mixture for measurements of residual activity. Curve fitting was carried out by nonlinear regression analysis, using a mono-exponential equation:

$$E_t = E_0\, e^{-k_{obs}t} \qquad (1)$$

where E_t and E_0 are enzyme activities at time t and zero time, respectively. The second-order rate constant of the inhibition was obtained by dividing k_{obs} by POX concentration.

Due to the rapid hydrolysis of DEP-2PAM, its inhibition rate constants were evaluated as previously described for the inhibition of AChE by the fast-hydrolyzing DEPC [16]. Briefly, 1–3 μM DEP-2PAM in deionized water (adjusted to pH 4.5) was diluted into the enzyme solution (1–2 nM) in the appropriate buffer that was preincubated at 29°, and residual enzyme activity was assayed after 10–15 min, by dilution into Ellman's mixture. As time increases, the ratio of the residual enzyme to its initial concentration (E_t/E_0) approaches a limiting value, as follows:

$$\ln E_\infty/E_0 = -[POX]_0\,(k_i/k_h) \qquad (2)$$

The end-point E_∞ was determined when enzyme activity did not change over 15 min. E_0 is the activity at zero time, and $[POX]_0$ is the initial concentration of DEP-2PAM. The second-order rate constant of the inhibition (k_i) was calculated from Equation 2 by using k_h values that were obtained as described below (see decomposition of POXs).

Preparation of DEP-ChE Conjugates

MoAChE or HuBChE (0.1 to 1.5 μM) in 10 mM Tris-0.1% BSA, pH 7.8, was incubated at 25° with paraoxon or DEP-4PAM at 10% excess above the stoichiometric amount of the enzymes. The decrease in enzymatic activity was monitored until inhibition was practically complete. To remove traces of unreacted OPs, 2 mL of the inhibited enzyme solution was dialyzed twice against 2 L of 10 mM Tris buffer, pH 7.8, for 48 hr at 5°.

Reactivation of DEP-ChE

The foregoing preparations were diluted in 10 mM Tris buffer-0.1% BSA, pH 7.8, to a final concentration as specified. At t = 0, stock solutions of 1–50 mM oximes in deionized water (adjusted to pH 7.8), were diluted into the inhibited enzyme that was preincubated at 29°. The rate of reactivation was followed by 30- to 300-fold dilution of the reactivation medium into the assay cuvette. Nonspecific hydrolysis of the substrate was subtracted. Reactivation in the presence of PTE was carried out as described above except that PTE in 10 mM Tris buffer-0.1% BSA, pH 7.8, was diluted into the inhibited enzyme prior to the addition of oximes.

Determination of K_m and k_{cat} of DEP-4POX

The equilibrium and rate constants of PTE-catalyzed hydrolysis of DEP-4POX were determined by measuring the initial velocity (first 0.5 min) of the release of 4-PAM at 336 nm. PTE activity was calculated from the molar extinction coefficient of 4-PAM in the assay medium. Spontaneous decomposition of DEP-4PAM was found to be negligible under the conditions described.

Decomposition of POXs

The identification of the decomposition products of DEP-OXs was based upon UV spectra, recorded with an HP8452A spectrophotometer (Hewlett Packard). Results were compared with spectra of standard solutions of authentic 2- and 4-CNPY. The decomposition rate constants (k_h) were determined independently by three procedures:

METHOD A. Direct measurements were based on the decrease in absorption at 282 and 252 nm for DEP-2PAM and DEP-4PAM, respectively. The decomposition rate constant, k_h, was calculated by using the following equation:

$$OD_t - OD_\infty = (OD_0 - OD_\infty)e^{-k_h t} \quad (3)$$

where OD_0, and OD_t, are the absorption at time zero and at time t, respectively. OD_∞ is the value assigned when no changes in absorption were observed over 15 min.

METHOD B. The time course of AChE inhibition was used to measure k_h of the fast-hydrolyzing DEP-2PAM, as previously described for DEPC [16]. At zero time, stock solution of DEP-2PAM (1–3 μM) in deionized water (adjusted to pH 4.5) was diluted 100-fold into the appropriate buffer, containing approximately 1.0 to 1.5 nM MoAChE or FBS-AChE. At time intervals of 7–25 sec, the inhibited enzyme solution was diluted into Ellman's mixture, and residual activity was assayed as described above. Each data point was obtained by a separate run, and k_h was calculated from the slope of the line plotted according to Equation 4 [16]:

$$\ln[\ln (E_t/E_0 - \ln (E_\infty/E_0)] = \ln \ln E_0/E_\infty - k_h t \quad (4)$$

where E_0, and E_t are the activity of AChE at zero time and at time t, respectively. E_∞ is the value assigned to AChE when no changes in enzyme activity were observed over 15 min.

METHOD C. Calculation of k_h of DEP-4PAM was also carried out by monitoring the loss of anti-ChE activity in the appropriate buffer solution. At various time intervals, approximately 1 μM POX solution was diluted 100-fold into 0.012 μM HuBChE in 10 mM Tris-0.1% BSA, pH 7.8. Residual POX was determined from the decrease in HuBChE activity after 15 min of incubation at 29°. The rate constant of the loss of anti-ChE of DEP-4PAM, that is assumed to correspond with k_h, was calculated from Equation 5:

$$[POX]_t = [POX]_0 \, e^{-k_h t} \quad (5)$$

where $[POX]_0$ and $[POX]_t$ are the inhibitor concentration at zero time and time t, respectively.

RESULTS

Synthesis and Configurational Analysis

The tertiary POXs, DEP-P2A and DEP-P4A (Fig. 1c, I and II, respectively), were obtained by reacting DEPC with the sodium salt of P2A and P4A by a procedure modified from van Hooidonk *et al.* [13]. Following removal of the major impurities, cyanopyridines and TEPP, the tertiary DEP-OXs were converted to the quaternary compounds by the use of DMSU. Based on absorption at 336 nm, both DEP-OXs contained, if any, less than 0.5% of 2- or 4-PAM. The exact concentration of stock solutions of the two POXs was verified by titration of a known concentration of HuBChE that was predetermined by DEPQ [12] (see below, Fig. 3C).

The structures of the two DEP-OXs were confirmed by NMR spectroscopy and MS measurements. The assignments of the ^1H, ^{31}P, and ^{13}C NMR resonances of the tertiary and quaternary DEP-OXs are shown in Table 1. In all cases, the NMR spectra suggested that only one kind of geometrical isomer was isolated. On the basis of comparing NMR chemical shifts and coupling constants with published values for *syn* and *anti* carboxaldehyde oximes [17–22], it was concluded that both DEP-OXs are the *syn* isomers (Fig. 1c). This assignment implies that the *syn* geometry of the starting materials P2A and P4A was maintained. The opposite orientation of the bulky pyridinium ring and the diethylphosphoryl moiety appears to stabilize DEP-OXs in the *syn* configuration.

Decomposition Products

UV spectra of 2- and 4-CNPY were well separated from the corresponding oximes (i.e. 2- and 4-PAM) (Fig. 2). Thus, based on spectral changes of DEP-2PAM and DEP-4PAM in near-neutral aqueous solutions, it was concluded that both DEP-OXs decomposed almost exclusively to the corresponding cyanopyridinium cations. When DEP-2PAM in stock solution (deionized water, pH 4.5) was transferred to 10 mM Tris buffer, pH 7.8, its conversion to 2-CNPY was complete within 1 min (Fig. 2A). The time course of the decomposition of DEP-4PAM to 4-CNPY was much slower (Fig. 2C). It was noted that in alkaline solutions, the main decomposition products of both DEP-OXs consisted of the corresponding pyridones and pyridinium carboxamides (not shown).

In the presence of PTE, the decomposition pattern of DEP-OXs changed markedly. DEP-4PAM was quantitatively converted to the parent oxime, 4-PAM (Fig. 2D). This was evident from (a) the molar absorbance coefficient at 336 nm; and (b) the ratio of absorption at 278 to 336 nm (2.8), which were similar to values obtained for authentic 4-PAM. By contrast, because of the rapid decomposition of DEP-2PAM, only a fraction of the expected amount of 2-PAM was released by PTE (Fig. 2B). The product ratio of oxime to 2-CNPY increased upon increasing the amount of the enzyme, suggesting a near-equal competition between the enzymatic and nonenzymatic reactions.

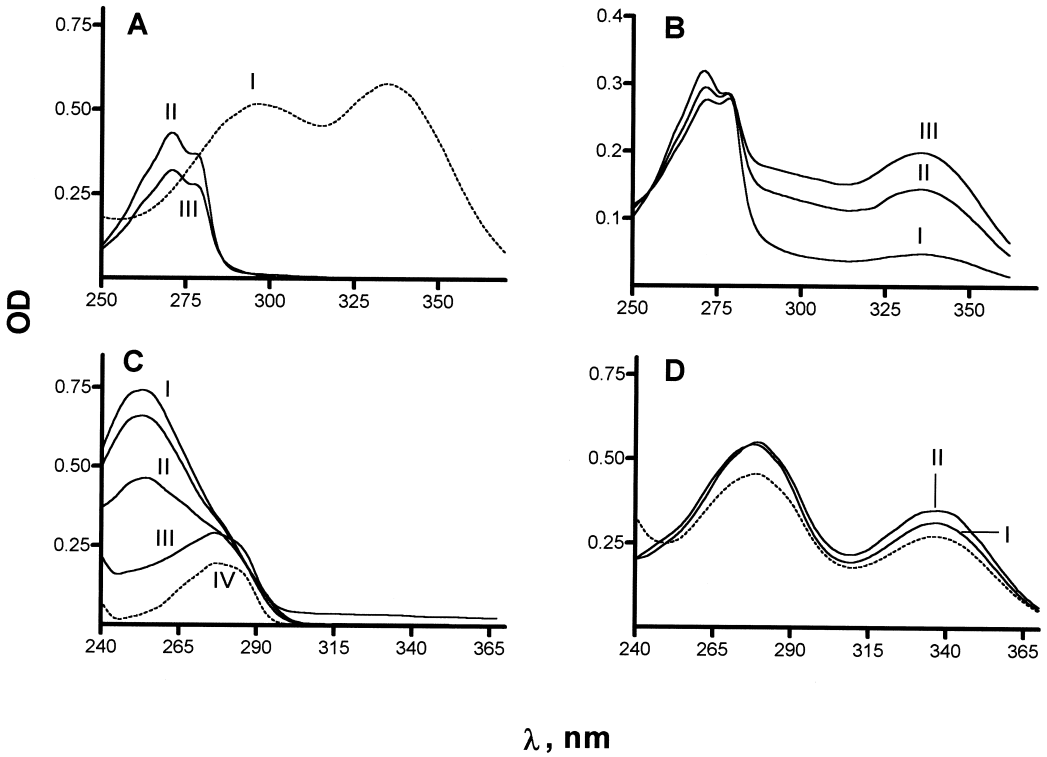

FIG. 2. UV absorption spectra of products of nonenzymatic decomposition and PTE-induced hydrolysis of DEP-OXs in 10 mM Tris buffer, pH 7.8. Panel A: I, 0.05 mM P2S; II, 0.05 mM authentic 2-CNPY; III, 0.04 mM DEP-2PAM. Panel B: 0.04 mM DEP-2PAM in the presence of increasing concentrations of PTE. I, 2.2 μg/mL of PTE; II, 5.5 μg/mL of PTE; III, 11 μg/mL of PTE. Panel C: Rate of conversion of 0.05 mM DEP-4PAM to 4-CNPY. I, 10 sec; II, 12 min; III, 60 min. IV, 0.04 mM authentic 4-CNPY. Panel D: 0.05 mM DEP-4PAM in the presence of: I, 0.53 μg/mL of PTE; II, 2.2 μg/mL of PTE. The dotted line is 0.04 mM authentic 4-PAM. The increase in absorption at 240 nm is due to the iodide of 4-PAM.

Stability in Aqueous Solutions

The four panels of Fig. 3 illustrate the determination of k_h according to Equations 3–5, and Table 2 summarizes half-life values of the decomposition of DEP-2PAM and DEP-4PAM in phosphate, Tris, and ADA buffers. k_h values obtained by three different protocols were found to be in reasonable agreement, suggesting that the conversion of DEP-OXs to 2- and 4-CNPY was accompanied by loss of anti-ChE activity. At pH 7.8, DEP-4PAM was found to be approximately 100-fold more stable than DEP-2PAM, and appeared to be less sensitive to the known general-base catalysis of phosphate buffer on certain OPs [23]. Thus, $T_{1/2}$ of DEP-2PAM in 5 mM phosphate decreased more than 2-fold relative to its stability in 10 mM Tris buffer, while only 20–30% acceleration of the decomposition of DEP-4PAM was observed upon its transfer from 10 mM Tris, pH 7.8, to 50 mM phosphate, pH 7.8.

Inhibition of ChEs

Titration showed that 1 mol of DEP-OXs was required to inhibit 100% of one active site of the enzyme (Fig. 3C). The second-order rate constants of the inhibition of AChEs and BChEs are summarized in Table 3. DEP-2PAM was found to be 35- and 140-fold more potent than DEP-4PAM as an inhibitor of MoAChE and FBS-AChE, respectively. This superiority decreased markedly, however, when BChEs from human and equine plasma were used. The largest second-order rate constants of DEP-2PAM (20.3×10^8 M^{-1} min^{-1}) and DEP-4PAM (7.1×10^8 M^{-1} min^{-1}) were observed with HuBChE. It was noted that the second-order rate constant of the inhibition of EqBChE by DEP-2PAM and DEP-4PAM decreased by 15- and 18-fold, respectively, compared with HuBChE. This points to structural differences between the catalytic site of the two enzymes.

Equilibrium and Kinetic Constants of PTE-Catalyzed Hydrolysis of DEP-4PAM

Table 4 compares K_m and k_{cat} of DEP-4PAM with those of paraoxon and DEPQ. K_m and k_{cat} were obtained from the standard Michaelis–Menten plot of the initial velocity of 4-PAM release versus the concentration of DEP-4PAM (not shown). k_{cat} was calculated assuming a molecular mass of 35 kDa [10]. The rapid decomposition of DEP-2PAM precluded accurate determination of K_m and k_{cat}. From the products ratio 2-PAM/2-CNPY under pseudo-first-order kinetics for both the enzymatic ($v = V_{max} \cdot K_m^{-1} \cdot [\text{DEP-2PAM}]$) and nonenzymatic reactions, it was estimated that k_{cat}/K_m of DEP-2PAM is $> 1 \times 10^7$ M^{-1} min^{-1} .

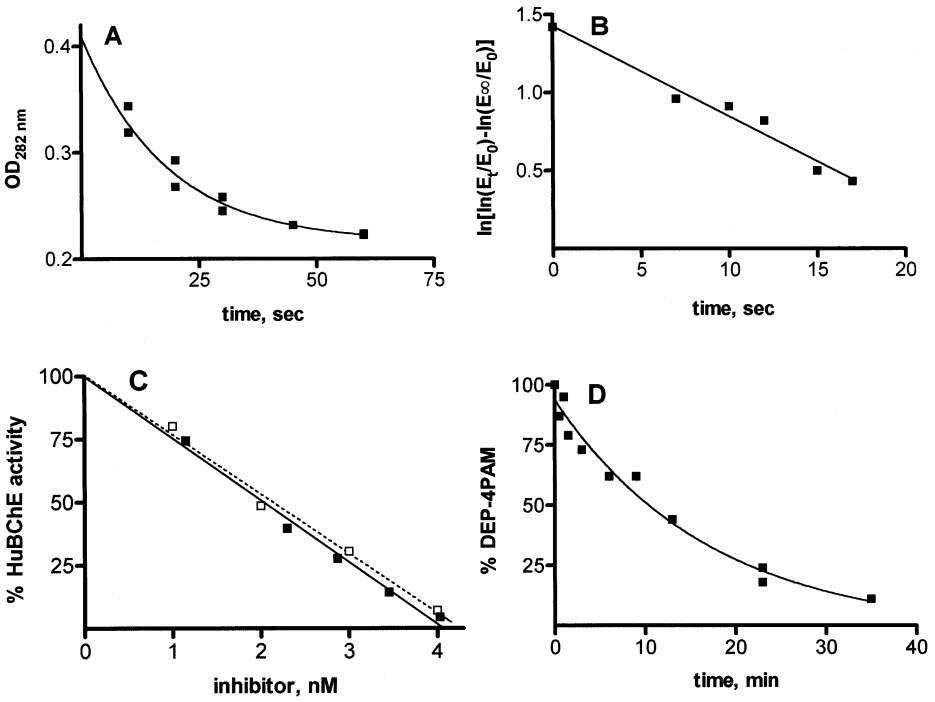

FIG. 3. Determination of the decomposition rate constants (k_h) of DEP-OXs by various methods. All measurements were carried out in 10 mM Tris buffer, pH 7.8, at 29°. Panel A: conversion of DEP-4PAM to 4-CNPY, determined from loss of absorbance at 282 nm. The curve was fitted to the data points according to a monoexponential decay equation. Panel B: Plot of the loss of enzyme activity induced by DEP-2PAM versus time, in accordance with Equation 4. Each data point represents a separate run. Panel C: Calibration curve of DEP-4PAM (■) obtained by titration of a known concentration of HuBChE that was predetermined by DEPQ (□). Panel D: Loss of anti-ChE potency of DEP-4PAM as determined by using the calibration curve shown in Fig. 3C. The curve was fitted to the data points according to Equation 5.

PTE-Enhanced Reactivation of DEP-ChEs by Oximes

In all cases reactivation of DEP-ChE conjugates exceeded 94% of the expected values.

MONO-QUATERNARY OXIMES. The second-order reactivation rate constant of DEP-MoAChE that was obtained by the use of the inhibitor DEP-4PAM (k_r of 2-PAM = 1387 ± 143 M^{-1} min^{-1}) was found to be similar to that reported for a DEP-MoAChE that was obtained by the use of paraoxon [10]. This suggests that DEP-OXs produced DEP-ChE conjugates. 2-PAM and 4-PAM are expected to generate DEP-2PAM and DEP-4PAM during reactivation of DEP-ChEs. Although the two DEP-OXs have been shown to be good substrates of PTE, reactivation of approximately 3 nM DEP-MoAChE by either oxime was not affected by PTE (Fig. 4, A and D). However, when the initial concentration of the inhibited enzyme increased by 100-fold, a marked enhancement of reactivation by 4-PAM was noted in the presence of 0.53 μg/mL of PTE (Fig. 4E), while reactivation by 2-PAM was affected only slightly, even when the PTE concentration was doubled (Fig. 4B).

TABLE 2. Half-lives of POXs in near-neutral aqueous solutions at 29°

POX	Buffer	pH	$T_{1/2}$*(sec)	Method†
DEP-2PAM	10 mM Tris	7.8	11 ± 3	A
		7.8	10 ± 3	B
		7.0	122 ± 24	A
	5 mM Phosphate	7.0	56 ± 12	A
	10 mM ADA	6.8	142 ± 22	A
		6.2	544 ± 44	A
DEP-4PAM	50 mM Phosphate	7.8	820 ± 91	A
		7.8	720 ± 57	C
	10 mM Tris	7.8	980 ± 108	A
		7.8	1020 ± 82	C

* Values are average (± SD) from 3–4 determinations.

†(A) Determined from changes in absorption at 282 and 252 nm for DEP-2PAM and DEP-4PAM, respectively. (B) Calculated from monitoring the rate of inhibition of AChE. (C) Determined from loss of anti-ChE activity. For further details, see Materials and Methods.

TABLE 3. Bimolecular rate constants of the inhibition of ChEs by phosphorylated oximes*

Enzyme source	DEP-2PAM†		DEP-4PAM	
	$k_i \times 10^{-8}$‡	Relative k_i	$k_i \times 10^{-8}$‡	Relative k_i
HuBChE	20.3 ± 5.4	15	7.1 ± 1.0	710
EqBChE	1.4 ± 0.5	1	0.4 ± 0.4	40
MoAChE	2.1 ± 0.2	1.5	0.06 ± 0.001	6
FBS-AChE	1.4 ± 0.2	1	0.01 ± 0.001	1

* Determined in 10 mM Tris buffer, pH 7.8, 29°.

†Obtained by using Equation 2.

‡M^{-1} min^{-1}. Values are averages ± SD (N = 4–6).

TABLE 4. Equilibrium and kinetic constants of DEP-4PAM and diethylarylphosphate hydrolysis by PTE from Pseudomonas sp*

OP	K_m (mM)	$k_{cat} \times 10^{-4}$ (min^{-1})	$k_{cat}/K_m \times 10^{-7}$ ($M^{-1}\,min^{-1}$)	Relative k_{cat}/K_m
DEP-4PAM	0.78	2.78	3.56	1
DEP-2PAM	ND†	ND	>1‡	
DEPQ§	0.079	2.38	30.1	8
Paraoxon§	0.032	4.45	139	39

*In 10 mM Tris, pH 7.8, 29°. Standard error is < 15%.
†Not determined.
‡Approximated from the product ratio 2-PAM/2-CNPY (see Results).
§From Ref. 10.

The dependency of PTE-enhanced reactivation of 4-PAM on the initial concentration of the inhibited enzyme can be explained by the prerequisite of sufficient DEP-4PAM to compensate for its relatively low k_i value (6.0×10^6 $M^{-1}min^{-1}$). By the same rationale, DEP-2PAM, despite its greater k_i (2.1×10^8 $M^{-1}min^{-1}$), did not produce significant inhibition of MoAChE because of its rapid decomposition. These considerations explain why the acceleration of the reactivation by PTE was greater with 4-PAM than with 2-PAM. To further substantiate these conclusions, reactivation of DEP-HuBChE was examined as described above for DEP-MoAChE. In the case of DEP-HuBChE, a 3 nM concentration of the inhibited enzyme was sufficient to demonstrate a PTE acceleration of reactivation by 4-PAM (Fig. 4F), but not by 2-PAM (Fig. 4C). The fact that the reactivation of DEP-HuBChE by 4-PAM is more amenable to acceleration by PTE than DEP-MoAChE is attributed to the k_i of DEP-4PAM versus HuBChE, which is 120-fold greater than with MoAChE. On the whole, although these observations reveal a complex dependency of the enhancement of reactivation on a variety of parameters, it is concluded that the stability of the DEP-OXs plays a dominant role in the capability of PTE to increase the apparent rate of reactivation.

BIS-QUATERNARY OXIMES. As observed with 4-PAM reactivation of 3 nM DEP-HuBChE, reactivation of 1.5 nM DEP-MoAChE by toxogonin and TMB-4 clearly deviated from a simple first-order reaction, and was enhanced by PTE in a concentration-dependent manner (Fig. 5, A and B). These reactivators contain the oxime function in position 4, and formally they are 4-PAM-based reactivators (Fig. 1). By contrast, acceleration of reactivation by HI-6, a 2-PAM-based oxime, was negligible in the same concentration of PTE (Fig. 5D). Reactivation by HLö7, which contains two oxime functions at position 2 and 4, also was enhanced by PTE (Fig. 5C). As observed with mono-quaternary oximes, these results show that the position of the DEP-OX moiety on the pyridinium ring of bis-quaternary reactivators largely dominates their responsiveness to PTE.

DISCUSSION

DEP-2PAM and DEP-4PAM represent two series of POXs that are likely to be produced during reactivation of DEP-ChEs with 2-PAM and 4-PAM-based reactivators (Fig. 1). The aim of this study was to characterize authentic DEP-2PAM and DEP-4PAM and to examine the role of their anti-ChE potency (k_i) and stability in aqueous solutions (k_h) on the time course of oxime-induced reactivation of DEP-ChEs. A second objective was to examine DEP-OXs as substrates of a PTE, and to evaluate its capacity to enhance reactivation by mono- and bis-quaternary oximes. Previously, characterization of diethylphosphoryl oximes has been based on *in situ* generation of POXs, and to our best knowledge this is the first reported synthesis of quaternary DEP-OXs.

Stability Studies and Nature of Decomposition Products

Hydrolysis of OP compounds usually occurs by a bimolecular displacement reaction at the phosphorus atom. Yet both DEP-OXs decomposed via the Beckman elimination mechanism to the 2- and 4-cyanopyridinium cations (Fig. 1d). These observations are consistent with the report of Steinberg and Solomon [24], who showed that a POX obtained by reacting sarin and 4-PAM decomposes to 4-CNPY. Alkaline hydrolysis of a tertiary DEP-OX (I, Fig. 1c) was reported to produce almost exclusively 2-cyanopyridine and diethylphosphoric acid [13]. This, together with the observation made with quaternary DEP-OXs, suggests that Beckman elimination was favored over substitution reaction regardless of the distance of the charge from the phosphorylated oxime moiety. The rate of the Beckman elimination reaction, however, depends on the location of the charged nitrogen relative to the POX function. The rapid decomposition of DEP-2PAM ($T_{1/2}$ = 10 sec), compared with DEP-4PAM ($T_{1/2}$ = 980 sec), is attributed mainly to the shorter distance between the charged pyridine nitrogen and the phosphorylated oxime moiety. The shorter the distance, the greater is the acidity of the methine proton and the electropositivity of the phosphorus atom, which facilitates the Beckman elimination reaction (Fig. 1d). The enhanced decomposition of DEP-OXs can be attributed, in part, to an intramolecular acid catalysis that involves protonation of a P=O (or P—O—C) bond by the methine hydrogen to form a six-membered ring intermediate (not shown).

The half-life of DEP-2PAM at pH 7.4 [37°] was estimated previously to be 26 sec, based on kinetic analysis of the reaction between O,O-diethylfluorophosphate and P2S [5]. The observed $T_{1/2}$ of DEP-2PAM (10 sec at pH 7.8, 29°) is in reasonable agreement with that calculated from results of *in situ* experiments. However, these values are substantially lower than a half-life of 69 min that was proposed on the basis of measuring P2S-induced reactivation of paraoxon-inhibited AChE [11], that is also expected to produce DEP-2PAM. Thus, the kinetic scheme of the

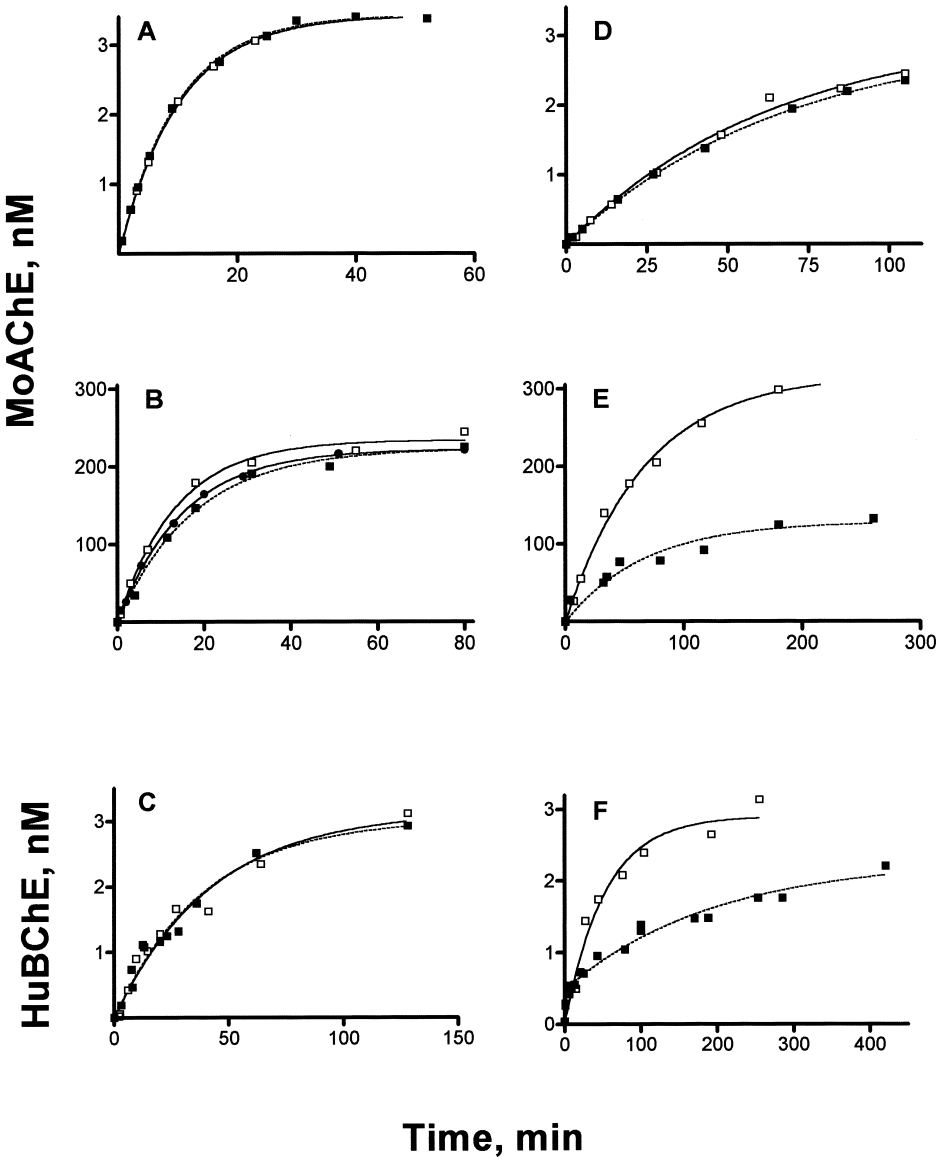

FIG. 4. Time course of PTE-induced reactivation of DEP-ChEs by 2- and 4-PAM in 10 mM Tris buffer, pH 7.8. Oxime concentrations were 0.1 and 0.5 mM for DEP-AChE and DEP-HuBChE, respectively. Key: ■, no PTE; and ● and □, reactivations in the presence of PTE. Dotted lines are reactivation time course in the absence of PTE. Panel A: 2-PAM versus 3 nM DEP-MoAChE. PTE = 0.53 μg/mL. Panel B: 2-PAM versus 250 nM DEP-MoAChE. □, PTE = 1.06 μg/mL. ●, PTE = 0.53 μg/mL. Panel C: 2-PAM versus 3 nM HuBChE. PTE concentration was increased to 2.96 μg/mL. Panel D: 4-PAM versus 3 nM DEP-MoAChE. PTE = 0.53 μg/mL. Panel E: 4-PAM versus 300 nM DEP-MoAChE. PTE = 0.53 μg/mL. Panel F: 4-PAM versus 3 nM DEP-HuBChE. PTE = 1.48 μg/mL.

various steps involved in the reactivation is most likely more complicated than previously thought.

PTE preferentially accelerated the substitution pathway, and the two oximes became the leaving groups of a displacement reaction at the phosphorus atom (Fig. 1d). Both PTE and ChEs are considered strong nucleophiles, and the remarkable deviation from the mechanism of the nonenzymatic decomposition implies that a high degree of molecular complementarity with the enzymes is involved. It is reasonable to assume that of the two pathways depicted in Fig. 1d, the substitution reaction is favored by the two hydrolases through stabilization of the transition state, a property that is unique to the architecture of the active sites of the two enzymes.

Inhibition of ChEs

The second-order rate constant of the inhibition of mouse AChE by DEP-2PAM ($2.1 \times 10^8\ M^{-1}\ min^{-1}$) is 1000-fold greater than the k_i of paraoxon [10], having *p*-nitrophenol as the leaving group (pK_a, 7.1)*, 35-fold greater than DEP-4PAM, having 4-PAM as the leaving group (pK_a, 8.6)*, and only 3.7-fold lower than the value reported for a diethylphosphate that contains 7-hydroxyquinolinium as the leaving group (DEPQ) [10].

The latter moiety is much more acidic (pK_a, 5.7) [25] than 2-PAM (pK_a, 8.07) [26], which is the leaving group of

* Unpublished results.

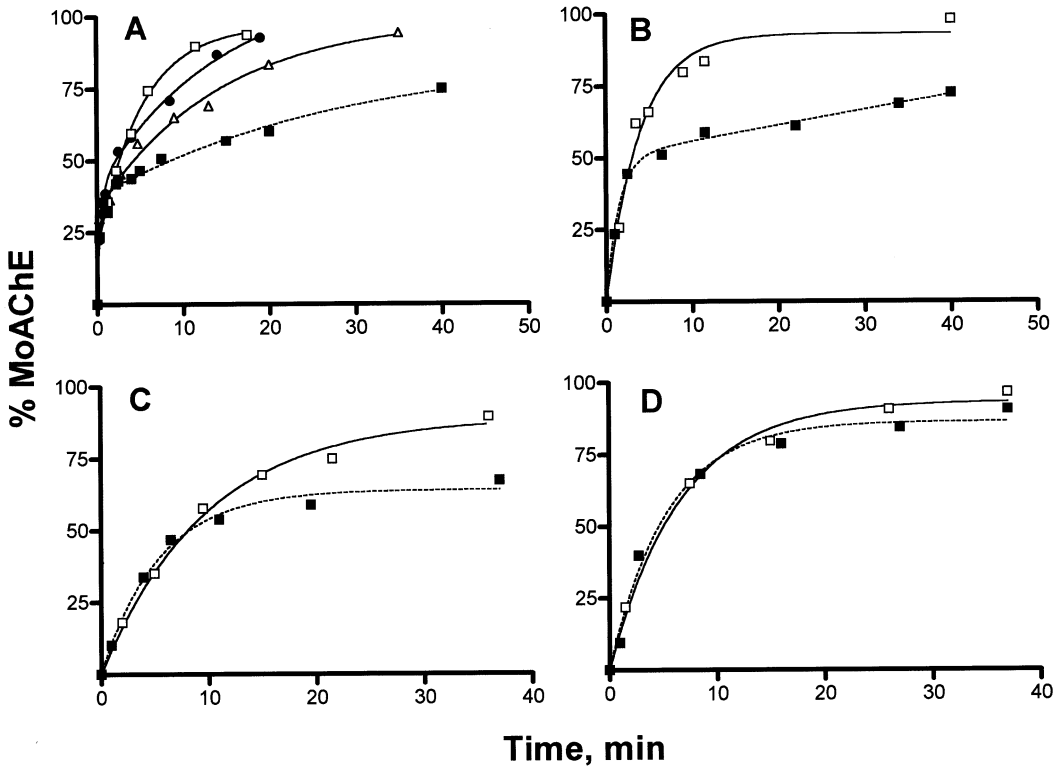

FIG. 5. Time course of PTE-induced reactivation of 1.5 nM DEP-MoAChE by bis-quaternary oximes in 10 mM Tris buffer, pH 7.8. Key: ■, no PTE, and □, reactivation in the presence of 1.48 μg/mL of PTE. Panel A: 0.01 mM toxogonin. Key: ●, PTE = 0.74 μg/mL; and Δ, PTE = 0.37 μg/mL. Panel B: 0.01 mM TMB-4. Panel C: 0.01 mM HLö7. Panel D: 0.3 mM HI-6.

DEP-2PAM. Thus, it is concluded that the increased reactivity of DEP-2PAM towards AChEs is largely due to structural features of the pyridinium oxime moiety rather than to the acidity of 2-PAM or to unusual changes in the electropositivity of the phosphorus atom. This peculiarity was even more pronounced with the exceptionally high second-order rate constant of the inhibition of HuBChE by DEP-2PAM and DEP-4PAM (20.3 and 7.1 $\times$ 10^8 M^{-1} min^{-1}, respectively). In fact, the enhanced anti-HuBChE potency is somewhat surprising. First, quaternary oximes commonly bind more tightly to, and reactivate OP-AChE conjugates faster than OP-BChE conjugates [26]. Second, the replacement of 6 of the 14 aromatic side chains that line the active site gorge of AChEs by smaller aliphatic amino acids in HuBChE [27], and presumably EqBChE, was expected to decrease cationic-π interactions with charged aromatic quaternary ligands. It is possible that the side chains of Trp 86 and Asp 74, which are conserved in AChEs and BChEs and have been shown to control the interaction of ChEs with charged ligands [28–30], and the enlarged size of the catalytic gorge of HuBChE [31], play a major role in the enhanced activity of the two POXs towards HuBChE.

Using FBS-AChE as a reference enzyme, the inhibition ranking order (Table 3) reveals that of the two DEP-OXs, the k_i of DEP-4PAM was increased towards HuBChE and EqBChE relative to the AChEs, much more than the k_i of DEP-2PAM. Considering the enlargement of the active site gorge of BChEs relative to AChEs, this observation suggests that DEP-4PAM exhibits larger steric constraints on the orientation of the POX in the active site of AChEs that would slow phosphorylation of the catalytic serine residue. It is of interest to point out that the k_i of both inhibitors was > 10-fold greater versus HuBChE than versus EqBChE. The observed change in energy barrier for the inhibition of HuBChE and EqBChE point to structural variations that are sufficient to produce significant differences in the reactivity of the two enzymes towards DEP-OXs.

Assuming that BChEs are serving as endogenous scavengers of OPs, these observations imply that species variations with oxime therapy may be linked, in part, to the rate of detoxification of POXs by the endogenous plasma BChE.

Kinetic analysis of a DEP-2PAM produced *in situ* resulted in a k_i that is > 19-fold lower against bovine AChE [5] than the k_i determined for authentic DEP-2PAM. This again points to the complicated kinetic scheme of the reactions that are involved in the formation and decomposition of POXs.

DEP-OXs as Substrates of PTE

The phosphotriesterase from *Pseudomonas* sp. rapidly hydrolyzed the two AChE inhibitors, suggesting that PTEs are reasonable candidates for acceleration of the detoxification of POXs. K_m and k_{cat} values of DEP-4PAM substantiated a previous report with respect to the ability of PTE to

hydrolyze effectively charged substrates that contain a quaternary aromatic moiety [10], as opposed to OPs with aliphatic ammonium alkylthiolate leaving groups [10, 32]. However, it is possible that the low k_{cat} values observed with phosphorothiolates (0.3 to 0.5 sec^{-1}) [32] are due to the nature of the P—S—alkyl bond rather than the positive charge on the side chain of the leaving group.

Ground-state affinity ranking order (K_m, Table 4) was found to be as follows: paraoxon (0.032 mM) > DEPQ (0.079 mM) > DEP-4PAM (0.78 mM). On the other hand, k_{cat} did not differ by more than a factor of 2. As noted with the inhibition of ChEs, the acidity of the leaving groups of the three substrates does not seem to play an important role in the catalysis by PTE. Thus, it is concluded that destabilization of the [PTE][substrate] complex (i.e. greater K_m values) shows a similar destabilization of the transition state, which can account for the observed decrease in k_{cat}/K_m of charged substrates. Yet it should be pointed out that PTE-catalyzed hydrolysis of DEP-4PAM is quite convincing. Calculations based on K_m and k_{cat} predict that at 37° 5 μg/mL of PTE will reduce the concentration of 10 nM DEP-4PAM to 0.01 nM in 1 min. Thus, relatively low concentrations of PTE can rapidly detoxify phosphorylated oximes and enhance reactivation, whenever the combination of $T_{1/2}$ and k_i of DEP-OXs is sufficient to produce significant reinhibition.

The inability of PTE to enhance 2-PAM reactivation is probably due to the rapid hydrolysis of DEP-2PAM, which suppressed its k_i value (35-fold greater than the k_i of DEP-4PAM). It should be pointed out that there is some uncertainty with respect to k_{cat}/K_m of DEP-2PAM, which also could explain the lack of enhancement of reactivation by PTE whenever 2-PAM or HI-6 was used. However, the estimated k_{cat}/K_m ($>1 \times 10^7$ M^{-1} min^{-1}) suggests that DEP-2PAM is as good a substrate as DEP-4PAM.

The characterization of k_i and k_h of authentic DEP-2PAM and DEP-4PAM provides a partial explanation for the well-established differences between the reactivation potencies of several bis-quaternary oximes (see Ref. 7). TMB-4 and toxogonin, being 4-PAM-based oximes, are expected to produce relatively stable DEP-OXs, which are likely to be potent inhibitors of AChE [4]. Indeed, PTE enhancement of DEP-AChE reactivation by the two oximes not only is consistent with this prediction, but also provides evidence that the putative POXs are substrates of PTE. On the other hand, the 2-PAM-based reactivator HI-6 is expected to be very unstable, reinhibition should be negligible, and, therefore, enhancement of reactivation by PTE will not be observed. The finding that reactivation by HLö7 was moderately, but markedly, affected by PTE raises the possibility that the oxime function in position 4 is involved in the reactivation of DEP-ChEs. These observations provide evidence for the hypothesis that the responsiveness of oxime reactivation to accelerating ligands such as edrophonium depends on the stability of the putative POX [7].

The reported lack of correlation between reactivation and antidotal potency has been attributed, in part, to therapeutic aspects of oximes that are unrelated to AChE reactivation [33–35]. To examine possible involvement of *in vivo* accumulation of POXs in such inconsistency, it will be necessary first to evaluate PTE as a prophylactic and therapeutic scavenger against the toxicity of POXs. This approach is based on the assumption that PTEs are present in mammalian tissues (e.g. paraoxonase). Thus, comparative evaluation of detoxification of authentic DEP-OXs by endogenous enzymes versus exogenously administered PTE is expected to clarify to what extent these inhibitors may interfere with *in vivo* reactivation.

CONCLUSIONS

Characterization of DEP-OXs has provided data that are considerably different from most reports that were based on *in situ* evaluations. In cases where the phosphorylated oxime decomposed rapidly, the bimolecular rate constant of the inhibition derived from *in situ* studies may be underestimated substantially. It would be of interest to analyze a modified kinetic scheme that will provide results approaching the k_i and k_h that were obtained for authentic DEP-2PAM and DEP-4PAM. Such a model could be employed more reliably for the investigation of POXs that are difficult to obtain in a purified state.

Finally, in view of current efforts to search for an AChE mutant scavenger of OPs that will be more amenable to reactivation then the wild-type enzyme [26, 36, 37], it would be worth considering potential implications of the formation of POXs. In that respect, coadministration of PTE, ChE, and a suitable oxime may offer a new lead for the search for antidotes against OP toxicity.

We thank Professor P. Taylor and Dr. Z. Radic for the donation of purified recombinant mouse AChE, Dr. B. P. Doctor for the purified FBS-AChE, and Dr. G. Amitai for the purified samples of HI-6 and HLö7.

References

1. Wilson IB and Ginsburg S, A powerful reactivator of alkylphosphate-inhibited acetylcholinesterase. *Biochim Biophys Acta* **18:** 168–170, 1955.
2. Hackley BE, Steinberg GM and Lamb JC, Formation of potent inhibitors of AChE by reaction of pyridinealdoximes with isopropyl methylphosphonofluoridate. *Arch Biochem Biophys* **88:** 211–214, 1959.
3. Lamb JC, Steinberg GM, Solomon S and Hackley BE, Isopropyl methylphosphonylated bisquaternary oximes; powerful inhibitors of cholinesterase. *Biochim Biophys Acta* **89:** 174–176, 1964.
4. De Jong LPA and Ceulen DI, Anticholinesterase activity and rate of decomposition of some phosphylated oximes. *Biochem Pharmacol* **27:** 857–863, 1978.
5. Harvey B, Scott RP, Sellers DJ and Watts P, *In vitro* studies on the reactivation by oximes of phosphylated acetylcholinesterase–I. On the reactions of P2S with various organophosphates and the properties of the resultant phosphylated oximes. *Biochem Pharmacol* **35:** 737–744, 1986.

6. Nenner M, Phosphonylated aldoximes. Inhibition of acetylcholinesterase and decomposition. *Biochem Pharmacol* **23:** 1255–1262, 1974.
7. Luo C, Ashani Y and Doctor BP, Acceleration of oxime-induced reactivation of organophosphate-inhibited fetal bovine serum acetylcholinesterase by monoquaternary and bisquaternary ligands. *Mol Pharmacol* **53:** 718–726, 1998.
8. Willems JL, De Bisschop HC, Verstraete AG, Declerck C, Christiaens Y, Vanscheeuwyck P, Buyalert WA, Vugelaers D and Colardyn F, Cholinesterase reactivation in organophosphorus poisoned patients depends on the plasma concentrations of the oxime pralidoxime methylsulphate and of the organophosphate. *Arch Toxicol* **67:** 79–84, 1993.
9. Hackley BE and Owens OO, Preparation of *O*-(isopropylmethylphosphono)-4- formyl-1-methylpyridinium iodide oxime. *J Org Chem* **24:** 1120, 1959.
10. Ashani Y, Leader H, Rothchild N and Dosoretz C, Combined effect of organophosphorus hydrolase and oxime on the reactivation rate of diethylphosphoryl-acetylcholinesterase conjugates. *Biochem Pharmacol* **55:** 159–168, 1998.
11. Schoene K, Reactivation of *O*,*O*-diethylphosphoryl-acetylcholinesterase. Reactivation-rephosphorylation equilibrium. *Biochem Pharmacol* **21:** 163–170, 1972.
12. Gordon MA, Carpenter DE, Barrett HW and Wilson IB, Determination of the normality of cholinesterase solutions. *Anal Biochem* **85:** 519–527, 1978.
13. van Hooidonk C, Kraaij GW and Ginjaar L, On the reactivity of organophosphorus compounds. Part IV. The alkaline hydrolysis of some *O*-phosphylated 2-pyridine oximes. *Rec Trav Chim* **87:** 673–686, 1968.
14. Grunwald J, Marcus D, Papier Y, Raveh L, Pittel Z and Ashani Y, Large scale purification and long-term stability of human butyrylcholinesterase: A potential bioscavenger drug. *J Biochem Biophys Methods* **34:** 123–135, 1997.
15. Ellman GL, Courtney KD, Andres V Jr and Featherstone RM, A new and rapid colorimetric determination of acetylcholinesterase activity. *Biochem Pharmacol* **1:** 88–95, 1961.
16. Ashani Y, Wins P and Wilson IB, The inhibition of cholinesterases by diethyl phosphorochloridate. *Biochim Biophys Acta* **284:** 427–434, 1972.
17. Boulet CA and Hansen AS, Synthesis and structure of some phosphonylated oximes related to organophosphate nerve agents. *Phosphorus Sulfur Silicon* **57:** 147–161, 1991.
18. Waysbort D, Balderman D and Amitai G, Carbon-13 NMR characterization of the bispyridinium oximes, toxogonin, HS-3, HS-6, and HI-6. *Org Magn Reson* **16:** 7–10, 981.
19. Pattison I and Wade K, Reactions between oximes and organo-derivatives of group III elements. Part II. Pyridine carboxaldehyde oxime. *J Chem Soc* (A): 2618–2622, 1968.
20. Poziomek EJ, Kramer DN, Mosher WA and Michel HO, Configurational analysis of 4-formyl-1-methylpyridinium iodide oxime and its relationship to a molecular complementarity theory on the reactivation of inhibited acetylcholinesterase. *J Am Chem Soc* **83:** 3916–3917, 1961.
21. Barfknecht CF and Westby TR, Conformationally and configurationally stabilized benzaldoxime. *J Pharm Sci* **58:** 490–491, 1969.
22. Karabatsos GJ and Taller RA, Structural studies by nuclear magnetic resonance XV. Conformations and configurations of oximes. *Tetrahedron* **24:** 3347–3360, 1968.
23. Levy D and Ashani Y, Synthesis and *in vitro* properties of a powerful quaternary methylphosphonate inhibitor of acetylcholinesterase: A new marker in blood-brain research. *Biochem Pharmacol* **35:** 1079–1085, 1986.
24. Steinberg GM and Solomon S, Decomposition of a phosphonylated pyridinium aldoxime in aqueous solution. *Biochemistry* **5:** 3142–3150, 1966.
25. Kitz RJ, Ginsburg S and Wilson IB, The reaction of acetylcholinesterase with diethylphosphoryl esters of quaternary and tertiary aminophenols. *Mol Pharmacol* **3:** 225–232, 1967.
26. Ashani Y, Radic Z, Tsigelny I, Vellom DC, Pickering NA, Quinn DM, Doctor BP and Taylor P, Amino acid residues controlling reactivation of organophosphonyl conjugates of acetylcholinesterase by mono- and bisquaternary oximes. *J Biol Chem* **270:** 6370–6380, 1995.
27. Cygler M, Schrag JD, Sussman JL, Harel M, Silman I, Gentry MK and Doctor BP, Relationship between sequence conservation and three-dimensional structure in a large family of esterases, lipases, and related proteins. *Protein Sci* **2:** 366–382, 1993.
28. Ordentlich A, Barak D, Kronman C, Flashner Y, Leitner M, Segall Y, Ariel N, Cohen S, Velan B and Shafferman A, Dissection of the human acetylcholinesterase active site determinants of substrate specificity. Identification of residues constituting the anionic site, the hydrophobic site and acyl pocket. *J Biol Chem* **268:** 17083–17095, 1993.
29. Hosea NA, Radic Z, Tsigelny I, Berman HA, Quinn DM and Taylor P, Aspartate 74 as a primary determinant of acetylcholinesterase governing specificity to cationic organophosphonates. *Biochemistry* **20:** 10995–11004, 1996.
30. Masson P, Froment MT, Bartels CF and Lockridge O, Importance of aspartate-70 in organophosphate inhibition, oxime reactivation and aging of human butyrylcholinesterase. *Biochem J* **325:** 53–61, 1997.
31. Saxena A, Redman AMG, Jiang X, Lockridge O and Doctor BP, Differences in active site gorge dimensions of cholinesterase revealed by binding of inhibitors to human butyrylcholinesterase. *Biochemistry* **36:** 14642–14651, 1997.
32. Rastogi VK, DeFrank JJ, Cheng T and Wild JR, Enzymatic hydrolysis of Russian-VX by organophosphorus hydrolase. *Biochem Biophys Res Commun* **241:** 294–296, 1997.
33. Clement JG, Efficacy of mono- and bis-pyridinium oximes versus soman, sarin, and tabun poisoning in mice. *Fundam Appl Toxicol* **3:** 533–535, 1983.
34. Rousseaux CG and Dua AK, Pharmacology of HI-6 and H-series oximes, *Can J Physiol Pharmacol* **67:** 1183–1189, 1989.
35. Van Helden HPM, de Lange J, Busker RW and Melchers BPC, Therapy of organophosphate poisoning in the rat by direct effects of oximes unrelated to ChE reactivation. *Arch Toxicol* **65:** 586–593, 1991.
36. Grosfeld H, Barak D, Ordentlich A, Velan B and Shaffernan A, Interactions of oxime reactivator with diethylphosphoryl adducts of human acetylcholiesterase and its mutant derivatives. *Mol Pharmacol* **50:** 639–649, 1996.
37. Saxena A, Maxwell DM, Quinn DM, Radic Z, Taylor P and Doctor BP, Mutant acetylcholinesterases as potential detoxification agents for organophosphate poisoning. *Biochem Pharmacol* **54:** 269–274, 1997.